MR Imaging of Brain Abscesses

Alison B. Haimes, Robert D. Zimmerman, Susan Morgello, Karen Weingarten, Richard D. Becker, Richard Jennis and Michael D. F. Deck

AJNR Am J Neuroradiol 1989, 10 (2) 279-291
http://www.ajnr.org/content/10/2/279

MR Imaging of Brain Abscesses

Alison B. Haimes[1]
Robert D. Zimmerman[1]
Susan Morgello[2]
Karen Weingarten[1]
Richard D. Becker[1,3]
Richard Jennis[1]
Michael D. F. Deck[1]

The MR images and CT scans of 14 patients with surgically verified pyogenic cerebral abscesses were reviewed. The MR findings correlated well with those seen on CT and were believed to be sufficiently characteristic to allow early and accurate diagnosis with MR alone. These features include (1) peripheral edema producing mild hypointensity on short TR/short TE and marked hyperintensity on long TR/intermediate to long TE scans; (2) central necrosis with abscess fluid hypointense relative to white matter and hyperintense relative to CSF on short TR/short TE scans and hyperintense relative to gray matter on long TR/intermediate to long TE scans (the fluid had concentric zones of varying intensity in seven cases, a finding not previously identified in other lesions); (3) extraparenchymal spread (intraventricular or subarachnoid), which was detected more easily on MR than on CT and was manifested by increased intensity relative to normal CSF on both short TR/short TE and long TR/intermediate TE scans; and (4) visualization of the abscess capsule, which was iso- to mildly hyperintense relative to brain on short TR/short TE scans and iso- to hypointense relative to white matter on long TR/intermediate to long TE scans. On the long TR scans, the relative hypointensity of the rim allowed for visualization of the typical morphologic features of the capsule, which in turn aided in differentiation of abscesses from other lesions (as it does on CT). To investigate the cause of the capsular intensity, pathologic studies of the capsules were reviewed when available (10 cases). Fibrosis was identified in all mature abscess capsules, but the combination of the intensities seen on short TR/short TE and long TR/intermediate to long TE scans as well as the temporal changes in intensity were believed to be incompatible with fibrosis as a cause of the capsular changes. Intensity patterns were suggestive of hemorrhage, but neither acute nor chronic hemorrhage was identified on routine H and E stains, while iron stain revealed scant hemorrhage in only two of the eight patients in whom these stains were used. We believe the capsular intensity (in particular the hypointense rims on long TR scans) may reflect paramagnetic T1, and to a greater extent T2, shortening, possibly due to the presence of heterogeneously distributed free radicals that are products of the respiratory burst produced by actively phagocytosing macrophages in the capsule wall.

Distinctive MR features of pyogenic abscesses should afford early and accurate diagnosis.

This article appears in the March/April 1989 issue of *AJNR* and the May 1989 issue of *AJR*.

Received July 13, 1988; accepted after revision October 25, 1988.

Presented at the Symposium Neuroradiologicum, Stockholm, June 1986.

[1] Department of Radiology, New York Hospital–Cornell Medical Center, 525 E. 68th St., New York, NY 10021. Address reprint requests to A. B. Haimes.

[2] Department of Pathology, New York Hospital–Cornell Medical Center, New York, NY 10021.

[3] Department of Radiology, Temple Medical Center, 40–60 Temple St., New Haven, CT 06510.

***AJNR* 10:279–291, March/April 1989**
0195–6108/89/1002–0279

Brain abscesses are potentially fatal lesions that may be treated successfully by medical and/or surgical intervention. Since the advent of CT, there has been a sharp decrease in the mortality of patients with parenchymal brain abscesses from greater than 40% to less than 5% [1–3]. The improved prognosis is attributed to early and accurate diagnosis and localization of these lesions, and to rapid detection of treatment failure and complications [1].

The role of MR imaging in these lesions has not been investigated extensively. The MR findings in 14 patients with pyogenic cerebral abscesses are described. One feature, a dark rim on long TR scans, is particularly notable. Histopathologic correlations are reviewed and a new potential mechanism for hypointensity due to T2 shortening is presented.

Materials and Methods

MR images of 14 patients (23 studies) with surgically verified pyogenic abscesses studied between September 1984 and May 1987 were analyzed retrospectively. In one patient (Case 13), postmortem examination was also performed. The clinical data are summarized in Table 1. In 10 cases, the clinical findings were suggestive of inflammatory disease (e.g., fever or leukocytosis), while the remaining four patients had nonspecific signs of a space-occupying mass. Ten patients were studied preoperatively; two of these were examined both pre- and postoperatively, one at less than 1 week and one at 1 year after surgery. Multiple lesions were identified in another patient (Case 7) in whom MR was performed after surgical drainage of the largest lesion. At least 10 smaller nonsurgical abscesses were identified in this study, the MR features of which were similar and were collectively considered a single preoperative case. Four patients were studied postoperatively only, two with serial scans, one within 1 week and another 1 year after surgical drainage.

MR was performed on a 0.5-T Teslacon unit* in 17 studies (nine preoperative, eight postoperative) and a 1.5-T Signa unit† in six studies (one preoperative, five postoperative). The axial plane was imaged routinely, and coronal and sagittal sections were obtained in selected cases. Slice thickness varied from 5 mm (1.5 T) to 7.5 mm (0.5 T). A variety of pulse sequences were used, particularly on the 0.5-T unit, due to periodic upgrades of these MR scanners. For purposes of comparison, sequences were divided into three groups within which MR images had similar intensities relative to normal CSF, gray matter, and white matter:

1. Short TR/short TE scans, 500–800/25–32/2 (TR/TE/excitations), in 12 patients (18 studies). On these images, which are considered T1-weighted for brain, CSF was dark, brain parenchyma was bright, and white matter was mildly hyperintense relative to gray matter.

2. Long TR/intermediate TE scans, 1500–2150/40–90/2, in 14 patients (22 studies). On these images, which are considered moderately T2-weighted, CSF was iso- to hypointense relative to white matter and moderately hypointense relative to gray matter.

3. Long TR/long TE scans, 2000–2150/80–120/2, in 14 patients (22 studies). On these images, which are considered heavily T2-weighted, CSF was hyperintense relative to brain.

Typically, multiecho scans were used to obtain long TR/intermediate TE and long TR/long TE scans, but interecho times varied from 30 to 60 msec and the number of echoes from two to four. One single-echo study (1500/90) was performed at 0.5 T (Case 4). Gradient-echo scans, 21/12/4 (TR/TE/excitations), were obtained at 1.5 T in three studies (two patients) with a 10° flip angle. One patient (Case 10) who was scanned at 0.5 T was evaluated before and after the IV injection of Gd-DTPA in a dose of 0.1 mmol.

In all 14 patients, routine CT scans were obtained on third-generation CT scanners. In 12 cases, studies were performed both before and after the administration of IV contrast material. One patient was studied only without contrast enhancement and one patient only after contrast enhancement.

Each lesion was evaluated on MR and compared with corresponding CT scans. Four regions were identified separately on the basis of CT findings and the known pathology of brain abscesses [2, 4–8]:

1. *Peripheral zone of edema*, corresponding to the extracapsular low-attenuation zone on CT. The intensity of this region was compared with that of brain parenchyma and CSF.

2. *Central zone*, corresponding to the central hypodensity within the abscess cavity on CT. The abscess fluid intensity was assessed with respect to CSF, gray matter, and surrounding edema on short TR/short TE and long TR/intermediate to long TE scans.

* Technicare, Cleveland, OH.
† General Electric, Milwaukee, WI.

TABLE 1: Clinical Characteristics of Pyogenic Cerebral Abscesses

Case No.	Age	Gender	Types and Timing of MR Studies	Histologic Findings of Biopsy Specimen
1	2	M	Postop 0.5 T (5 days, 2 weeks) Postop 1.5 T (6, 8, 10, 15 weeks)	Cultured only; no histology
2	10	M	Preop 0.5 T	Organizing abscess with diffuse macrophages
3	24	F	Postop 0.5 T (1 year)	Cultured only; no histology
4	28	F	Preop 0.5 T	Mature abscess capsule; moderate macrophages
5	39	M	Preop 1.5 T	Organizing abscess; focal sheets of macrophages
6	40	M	Preop 0.5 T	Multifocal acute cerebritis with early abscess and scattered macrophages
7	47	M	Preop 0.5 T Postop 0.5 T (1 week)	Granulation tissue with focal necrosis, macrophages
8	52	F	Preop 0.5 T	Cultured only; no histology
9	59	F	Postop 0.5 T (1 week)	Acute cerebritis; early abscess formation with leukocytes and macrophages
10	60	F	Preop 0.5 T Postop 1.5 T (1 year)	Organizing abscess with granulation tissue and diffuse macrophages
11	64	F	Postop 0.5 T (9 days, 5 weeks)	Granulomatous infiltrate with occasional giant cells and focal necrosis
12	65	F	Preop 0.5 T Postop 0.5 T (1 week)	Cultured only; no histology
13	65	F	Preop 0.5 T	Organizing abscess with granulation tissue; sheets of lipid-laden macrophages
14	70	M	Preop 0.5 T	Organizing abscess extending into choroid plexus, with granulation tissue and sheets of lipid-laden macrophages

Note.—Preop = preoperative; postop = postoperative.

3. *Extraparenchymal spread*. Abscess extension was evident by areas of abnormal intensity within adjacent CSF spaces.

4. *Abscess capsule*. The configuration and intensity of the rim of tissue interposed between the peripheral edema and central necrosis were evaluated. Because this fell within the confines of the region of ring enhancement on CT it was believed to represent the abscess capsule.

The intensity of each MR rim was compared with that of frontal gray and white matter on short TR/short TE scans and was graded on long TR/intermediate to long TE scans as follows (Table 2): grade I—iso- to minimally hyperintense relative to frontal white matter and hypointense relative to gray matter; grade II—moderately hypointense relative to frontal white matter, iso- or mildly hyperintense relative to the splenium of the corpus callosum, and hypointense to gray matter; and grade III—moderately to markedly hypointense relative to all white and gray matter. In addition, rim intensities were compared with the intensity of the posterior aspect of the falx cerebri.

All 14 abscesses were surgically drained and cultured. Ten abscess capsule specimens were available for review. The location of seven of the 10 biopsy sites was known from surgical reports and/or postoperative imaging studies. All 10 were routinely evaluated by light microscopy with H and E stains. Each specimen was evaluated for the presence of acute or chronic hemorrhage as manifested by extravascular erythrocytes or hemosiderin-laden macrophages, respectively. Eight specimens were restained with Gomori's modification of Perls' stain for ferric forms of iron. Gram stains for bacteria, Gomori's methenamine silver stain for fungus, Masson stains for collagen, and acid-fast stains for mycobacteria were also used. The abundance of macrophages on H and E stains was graded: grade I—scattered macrophages, *grade II*— moderate macrophages, and grade III—diffuse macrophages (Table 3).

To further evaluate the causes of hypointensity on MR, three additional patients were reviewed. Their lesions, one tuberculoma and two metastases, demonstrated hypointensity on long TR/intermediate to long TE scans and were pathologically evaluated in the same manner as the abscesses.

Results

The preoperative MR examination of pyogenic cerebral abscesses revealed discrete lesions in all 10 patients. Irregularly marginated subtle hypointensity with respect to brain on short TR/short TE scans (Fig. 1C) and marked hyperintensity on long TR/intermediate to long TE images (Figs. 1–4) correlated well with the hypodense peripheral edema seen on CT. Although the contrast between edema and surrounding tissues was more marked on long TR/intermediate to long TE scans than on CT scans, edema was always well visualized on CT scans.

TABLE 2: Grades of Rim Intensity of Pyogenic Cerebral Abscesses on Long TR/Intermediate TE and Long TR/Long TE MR Images

Grade	No. of Findings		
	Preoperative MR	Postoperative MR	
		1 Week	1–4 Weeks
I	4[a]	1	1
II	3	3	1
III	2	0	0
Total	9	4	2

Note.—Grade I = iso- to hyperintense relative to frontal white matter and hypointense relative to gray matter; grade II = hypointense relative to white matter, iso- to hyperintense relative to splenium of corpus callosum, and hypointense relative to gray matter; grade III = hypointense relative to all white and gray matter.

[a] In one patient with surgically and pathologically proved acute cerebritis, the entire lesion was of grade I intensity.

TABLE 3: Comparison of Rim Intensities and Histologic Findings in Pyogenic Cerebral Abscesses

Case No.	Grade of Rim Intensity[a]	Grade of Macrophage Infiltration[b]	Presence of Hemorrhage or Iron in Abscess Capsule	
			H and E	Iron Stain
1	II	Histology not performed		
2	II	III	None	None
3	–[c]	Histology not performed		
4	II	II	None	Not performed
5	III	III	None	Not performed
6	I	I	None	None
7	II	II	None	None
8	II	Histology not performed		
9	I	II	None	None
10	I	III	None	Focal/scant
11	II	II	None	None
12	II	Histology not performed		
13	III	III	None	Focal/scant
14	I	III	None	None

[a] Grade was determined on long TR images in the initial patient study. Intensity grades are defined in Table 2.

[b] Grade I: scattered macrophages; grade II: moderate macrophagic infiltrate; grade III: diffuse macrophages, some in sheets.

[c] Scan obtained 1 year postoperatively; no discrete lesion was seen.

The signal intensity of the central area corresponding to the abscess cavity on CT was intermediate between that of CSF and brain on all short TR/short TE scans (Fig. 1C). Abscess fluid intensity was consistently greater than that of CSF and was equal to that of gray matter in five of eight cases on long TR/intermediate TE scans (Fig. 3B) and greater than that of gray matter in three cases (Fig. 2C). The signal intensity of the abscess fluid increased as TE was prolonged. Of 10 long TR/long TE scans, one showed fluid intensity equal to that of gray matter, six showed intensity between that of gray matter and edema (Fig. 3C), and the remaining three showed fluid intensity equal to that of edema (Fig. 2D). While central material was homogeneously hypodense (iso- or slightly hyperdense relative to CSF) on CT, this region showed concentric alternating zones of relative hypo- and hyperintensity on seven of 10 MR scans (Figs. 1D and 2E). This appearance was subtle in smaller lesions but became more marked in large abscesses.

Two cases of extraparenchymal abscess extension were noted on preoperative MR, but not on CT. In both cases, intensity was increased relative to CSF, in particular on long TR/intermediate TE scans, while the infected fluid remained isodense relative to CSF on CT. These included one case of surgically confirmed intraventricular extension (Figs. 3A and 3C) and one case of autopsy-confirmed spread into the quadrigeminal plate cistern (Figs. 1B–1D).

In preoperative studies a discrete rim was identified at the margin of the central necrotic zone on both short TR/short TE (seven of nine cases) and long TR/intermediate to long

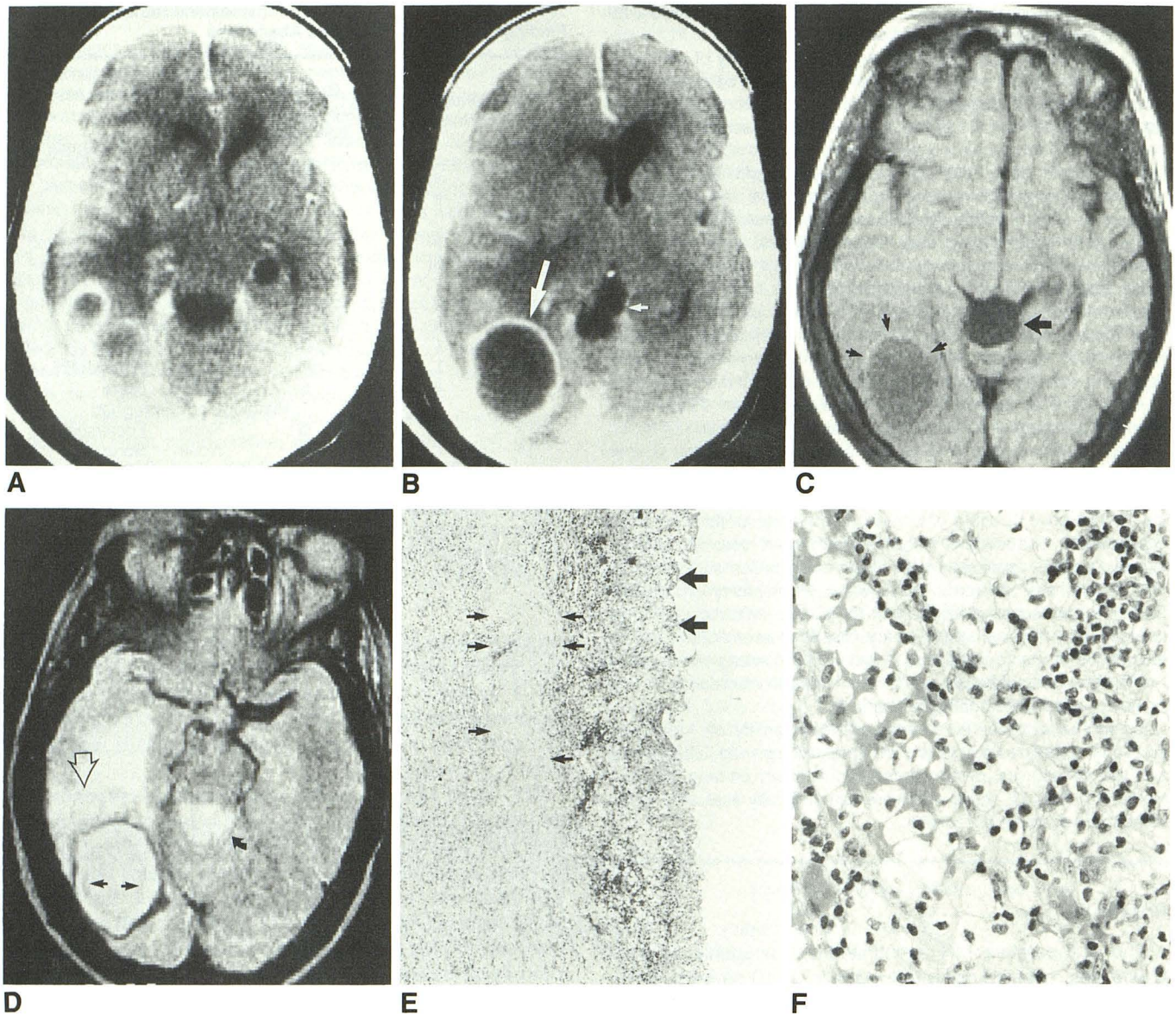

Fig. 1.—Case 13: Preoperative brain abscess.

A and *B*, CT scans show ring-enhancing lesion in right occipital lobe with adjacent edema. Multiloculation is apparent (*A*). Note typical mesial wall thinning (*large arrow*). Quadrigeminal plate cistern (*small arrow*) is prominent but otherwise normal.

C, MR image, 500/32 (0.5 T), shows central abscess cavity material as hypointense relative to white matter and hyperintense relative to normal CSF in lateral ventricles (not shown). Subtle hyperintense rim is seen at margin (*small arrows*). Minimal hypointensity in adjacent brain represents edema. Fluid within quadrigeminal plate cistern is subtly hyperintense relative to CSF but less intense than abscess fluid (*large arrow*).

D, MR image, 2150/64 (0.5 T), shows central area that is hyperintense relative to gray matter and CSF and slightly hypointense relative to edema. More peripherally within abscess cavity, material appears more hyperintense, and zone of relative hypointensity (*straight solid arrows*) is seen between these regions producing concentric rings of variable signal. Dramatic hypointense rim (grade III) is seen within abscess capsule. Small loculation (*open arrow*) corresponds to that seen on CT (*A*). Adjacent edema is hyperintense. Note hyperintensity within quadrigeminal plate cistern (*curved arrow*).

E, Photomicrograph of abscess wall shows granulation tissue, dense fibrous tissue (*small arrows*), and numerous lipid-laden macrophages (*large arrows*). (H and E stain, original magnification ×63)

F, High-power photomicrograph shows lipid-laden macrophages and lymphocytic infiltrate. No evidence of acute or chronic hemorrhage is present (H and E, original magnification × 400)

TE (nine of 10 cases) scans. On short TR/short TE scans the rim was mildly hyperintense relative to white matter in four cases (Fig. 1C) and isointense (delineated by adjacent hypointense peripheral edema and central necrosis) in three cases (Fig. 4A). On long TR/intermediate to long TE scans, the rim was hypointense relative to gray matter in all nine cases. It was hypointense (five cases, e.g., Figs. 1D and 2C–2E) to isointense (four cases, e.g., Figs. 3B, 3C, 4B, and 4C) relative to white matter and became darker as TE was prolonged (Table 2). One patient with surgically and pathologically confirmed acute cerebritis did not have a discrete rim on short TR/short TE or long TR/intermediate to long TE scans. This lesion was diffusely isointense relative to brain on short TR/short TE scans and isointense relative to white matter (grade I) on long TR/intermediate to long TE scans. The location and configuration of the dark rim on long TR/intermediate to long

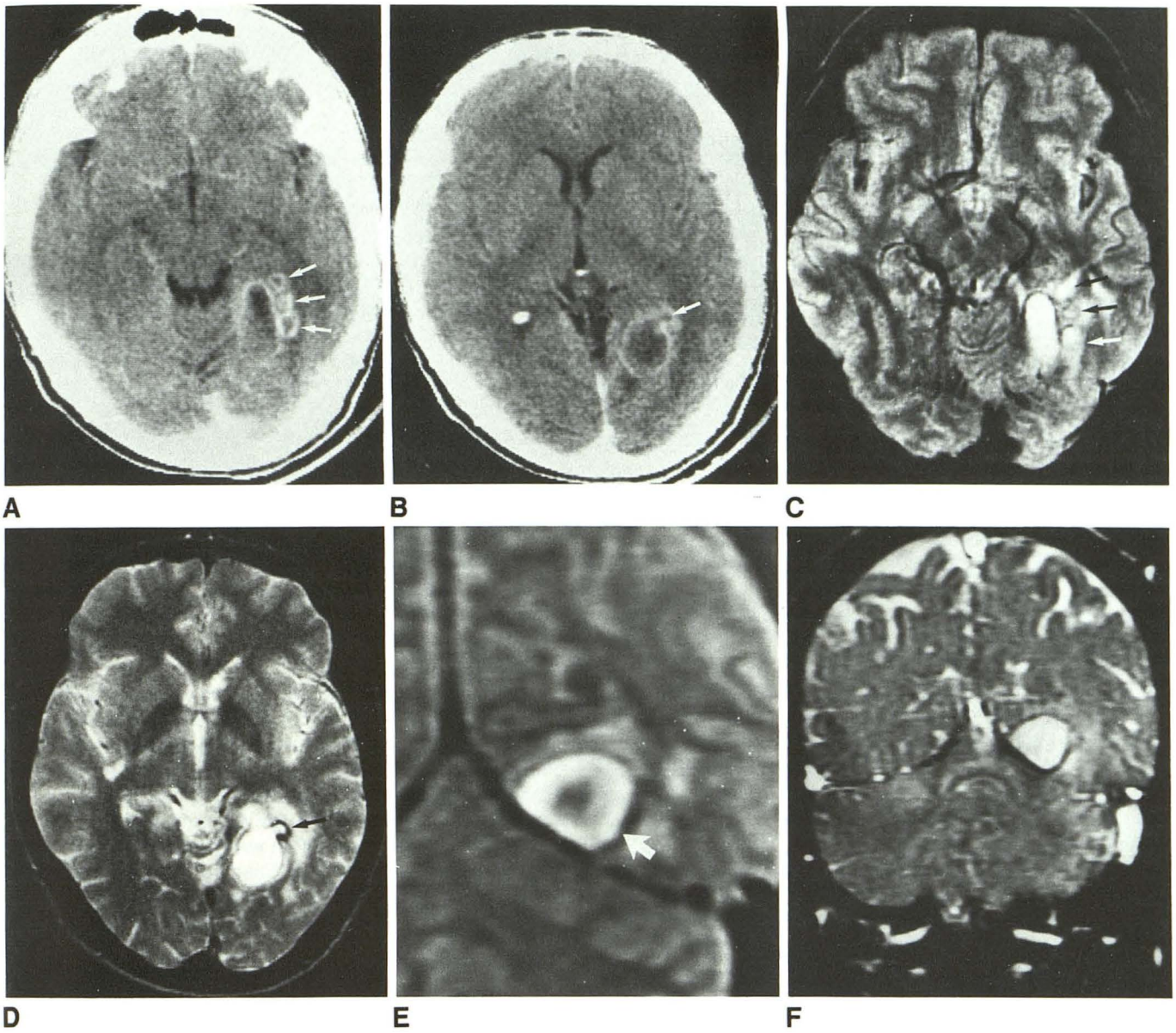

Fig. 2.—Case 5: Preoperative brain abscess.

***A* and *B*, Contrast-enhanced CT scans in chronic abscess show large enhancing ring lesion with minimal edema. Note three satellite foci inferiorly (*arrows, A*) and single, "budlike" projection superiorly (*arrow, B*).**

***C* and *D*, MR images, 2000/40 (*C*) and 2000/80 (*D*) at 1.5 T, show excellent correspondence. Grade III hypointense rim surrounds abscess, three satellite foci (*arrows, C*), and bud (*arrow, D*).**

***E*, Magnified view of coronal image 2000/40 (1.5 T) shows concentric rings in abscess center. Biopsy site is known (*arrow*) from surgical notes and is hypointense.**

***F*, Rim is hypointense also on gradient-echo image, 21/12 (10° flip angle) at 1.5 T.**

TE scans closely matched the enhanced ring visualized on CT; the short TR/short TE rim correlated less well. Subtle loculations and small satellite lesions were seen in all four cases in which these were identified on CT (Figs. 1–3).

The postoperative patients were evaluated on the basis of time from surgical intervention. Evaluation of the four studies performed within 1 week of surgery revealed features similar to the preoperative cases, including peripheral edema, central abscess fluid, and a discrete rim (Figs. 5B, 6A, and 6B). Mild hyperintensity on short TR/short TE scans was noted in the abscess cavity in two cases with evidence of increased central density on CT, probably indicative of postoperative hemorrhage. The presence of the dark rim allowed visualization of the morphologic characteristics of the abscess, which corresponded well to concurrent CT findings. The intensity of the rim did not change significantly in the one patient studied just before and after surgical drainage (Figs. 5B and 5C), nor was there a significant alteration of intensity when all preoperative and early postoperative cases were compared (Table 2).

More delayed follow-up studies (9 days to 1 year) were available in four patients (nine studies) and showed progressively decreasing edema, mass effect, and abscess cavity

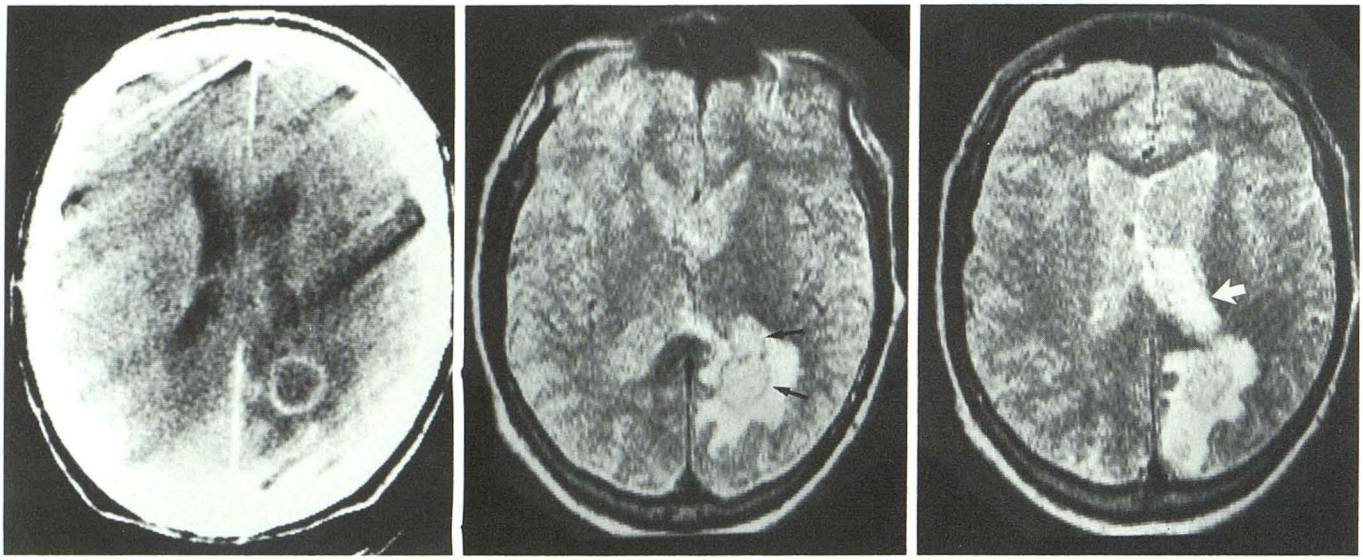

Fig. 3.—Case 14: Preoperative brain abscess.

***A*, Motion-degraded contrast-enhanced CT scan shows ring-enhancing left occipital abscess with mesial wall thinning. Intraventricular spread cannot be identified.**

***B* and *C*, MR images, 2150/64 (*B*) and 2150/96 (*C*) at 0.5 T, show multilocular lesion with grade I rim intensity (*arrows, B*) and intraventricular extension of abscess with involvement of choroid plexus (*arrow, C*). Note hypointensity of falx cerebri.**

size. In one patient (Case 11) serial postoperative studies showed progressive diminution of the abscess rim hypointensity. In another patient (Case 1) rim hypointensity decreased between the 5-day and 2-week scans (both obtained at 0.5 T; Figs. 6B and 6C), while a follow-up study at 6 weeks at 1.5 T showed an increase in rim hypointensity without a change in clinical status (Fig. 6D). Further sequential studies up to 15 weeks at 1.5 T revealed complete resolution of the hypointense rim and central necrotic cavity (Fig. 6E). In both serially evaluated patients, contrast-enhanced CT scans obtained close in time to the MR studies continued to demonstrate an enhancing ring. Late follow-up studies at 1 year (Cases 3 and 10, Figs. 4F and 4G) demonstrated only subtle hypointensity on short TR/short TE scans and focal hyperintensity on long TR/long TE scans, without mass effect.

Histopathologic evaluation of the 10 pyogenic abscess biopsy specimens revealed a spectrum of the stages of abscess evolution (Table 1). These include (1) two patients with acute cerebritis or early abscess formation (Cases 6 and 9); (2) seven patients with organizing abscesses (Cases 2, 4, 5, 7, 10, 13, and 14) characterized by granulation tissue containing capillaries, fibroblasts, macrophages, lymphocytes, and polymorphonuclear cells; and (3) one patient (Case 10) with a chronic abscess with a granulomatous infiltrate and foci of necrosis. Macrophages, which were diffusely distributed throughout the capsules of the organizing abscesses, had abundant cytoplasm that ranged from eosinophilic to vacuolated in appearance (Figs. 1E and 1F). Large discrete collections of lipid-laden macrophages were seen in two patients (Cases 13 and 14). Macrophagic infiltration ranged from grade II to III in mature and chronic abscesses and was grade I only in a patient with cerebritis (Table 3). Neither extravascular erythrocytes nor iron pigment was detected by H and E stains in any of the 10 biopsy specimens. Iron stains were performed in eight of 10 specimens. No iron was detected in six specimens, while scant, focal iron deposition was present in only two abscess capsules, one with grade I (Case 10) and one with grade III (Case 13) rim intensity on long TR/intermediate to long TE scans. (Iron was present in the inflamed choroid plexus of one patient [Case 14] and in the leptomeninges of another [Case 9].) Collagen was present in all organizing and chronic abscesses, but was not seen in the cases of cerebritis.

MR and pathologic evaluations of the three patients without pyogenic abscess were performed. One tuberculous granuloma was diffusely hypointense (grade III) on long TR/intermediate to long TE scans. The two metastatic foci had rim appearances similar to those of the majority of the abscesses, including grade II hypointensity of the rim on long TR/intermediate to long TE images (Figs. 7B and 7C). Pathologic evaluation of the tuberculoma revealed granulation tissue with fibroblasts, capillaries, and grade II macrophagic infiltration. In both cases of metastatic carcinoma, the neoplasms were surrounded by sheets of lipid-laden macrophages (grade III), scattered lymphocytes, and proliferating vessels (Fig. 7D). Collagen was not a feature of the metastatic lesions. No hemorrhage or iron was detected in the tuberculoma or the metastatic carcinomas.

On microbacteriologic evaluation, a variety of organisms was cultured. In four cases, two organisms were identified. The most prevalent bacteria were *Streptococcus milleri* and *Peptostreptococcus*, each seen in three cases. No organisms were cultured in two patients in whom antibiotic therapy had been initiated long before surgery.

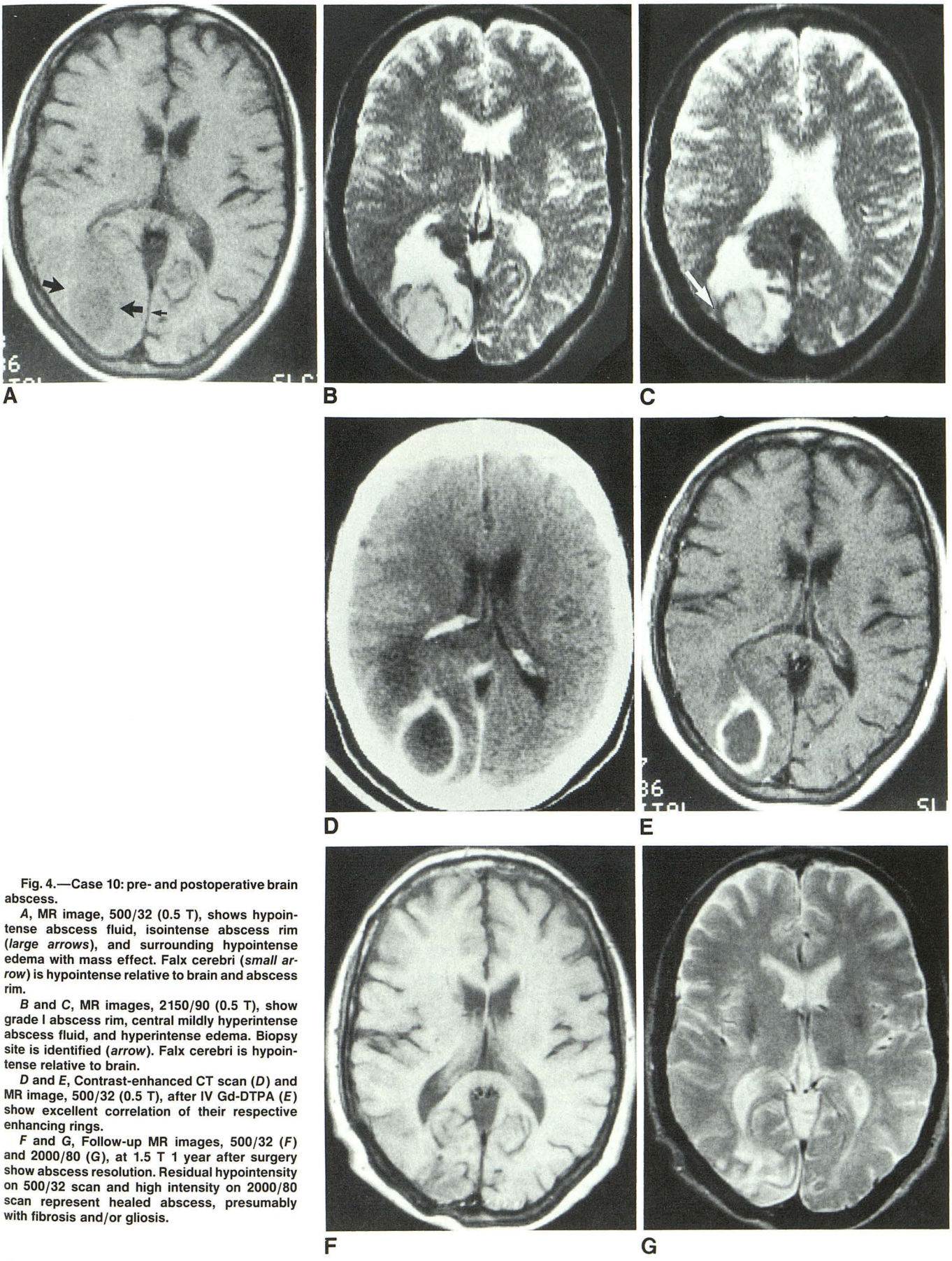

Fig. 4.—Case 10: pre- and postoperative brain abscess.

A, MR image, 500/32 (0.5 T), shows hypointense abscess fluid, isointense abscess rim (*large arrows*), and surrounding hypointense edema with mass effect. Falx cerebri (*small arrow*) is hypointense relative to brain and abscess rim.

B and *C*, MR images, 2150/90 (0.5 T), show grade I abscess rim, central mildly hyperintense abscess fluid, and hyperintense edema. Biopsy site is identified (*arrow*). Falx cerebri is hypointense relative to brain.

D and *E*, Contrast-enhanced CT scan (*D*) and MR image, 500/32 (0.5 T), after IV Gd-DTPA (*E*) show excellent correlation of their respective enhancing rings.

F and *G*, Follow-up MR images, 500/32 (*F*) and 2000/80 (*G*), at 1.5 T 1 year after surgery show abscess resolution. Residual hypointensity on 500/32 scan and high intensity on 2000/80 scan represent healed abscess, presumably with fibrosis and/or gliosis.

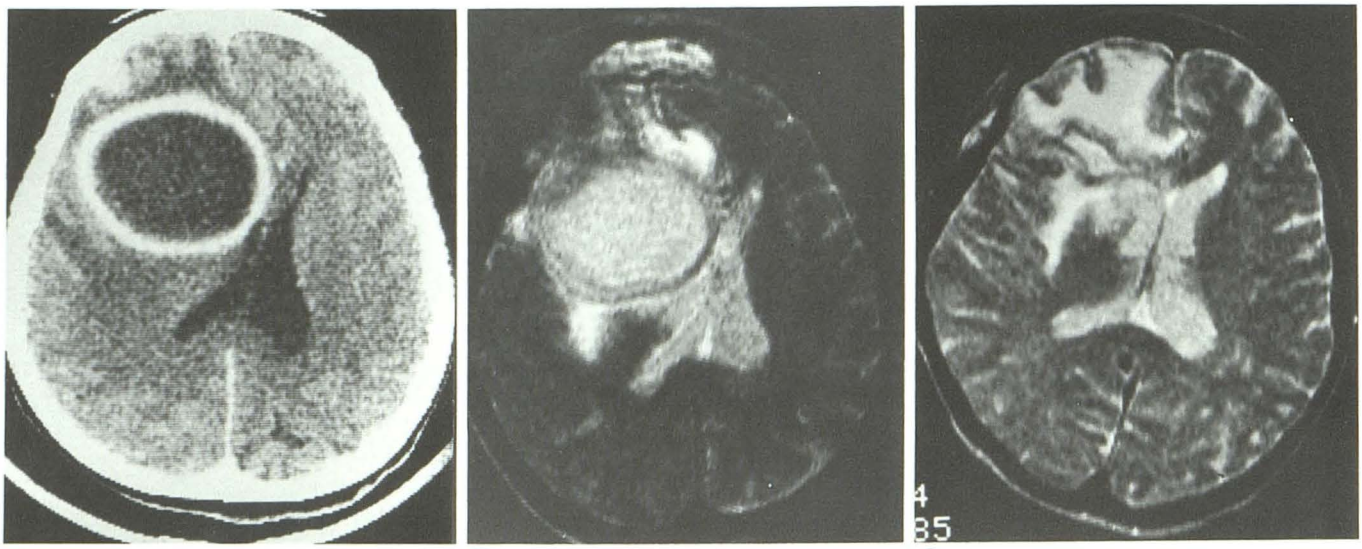

Fig. 5.—Case 12: Pre- and postoperative chronic brain abscess.
***A*, Contrast-enhanced CT scan reveals thick-walled chronic abscess.**
***B*, Motion-degraded MR image, 2150/60 (0.5 T), shows grade II rim intensity.**
***C*, Follow-up image, 2150/60 (0.5 T), within 1 week of drainage shows collapse of abscess capsule comparable to that seen on CT (not shown). There is no significant change in grade of rim hypointensity when compared with preoperative scan.**

Discussion

During the past decade, CT has proved to be an excellent technique for the evaluation of intracranial abscesses, and has been a major factor in the improved survival and reduced mortality now associated with these lesions [1–3]. A constellation of CT features that differentiate abscesses from primary and metastatic neoplasms, infarction, and noninfectious inflammatory lesions is based on pathologic findings and includes (1) peripheral hypodensity due to edema, (2) central hypodensity due to necrosis, (3) intraventricular hyperdensity and/or periventricular enhancement due to extraparenchymal spread, and (4) a highly characteristic pattern of ring enhancement reflecting the unique pathogenesis of the abscess capsule [2, 4–8]. Review of the cases in this series indicates that MR is valuable for detecting and characterizing brain abscesses by demonstrating features corresponding to the CT findings as well as additional features not seen on CT.

Mild hypointensity on short TR/short TE images and marked hyperintensity on long TR/intermediate to long TE images were noted surrounding all preoperative and early postoperative abscesses, reflecting prolongation of T1 and T2 relaxation times due to vasogenic edema [9]. Though edema was identified on CT in every case, contrast between edema and adjacent brain was higher on MR than on CT due to the greater sensitivity of MR to changes in tissue water content (Figs. 1–4) [9]. This might offer a potential advantage in the detection of subtle edema in the early stages of abscess evolution. Serial MR scans showed resolution of hypointensity on short TR/short TE scans and a decrease in the extent of hyperintensity on long TR/intermediate to long TE scans 1–2 months after surgical drainage, indicative of decreasing edema (Fig. 6).

The abscess center demonstrated hyperintensity relative to CSF and hypointensity relative to white matter on short TR/short TE images, hyperintensity relative to CSF and iso- to hyperintensity relative to gray matter on long TR/intermediate images, and iso- to mild hyperintensity relative to CSF and gray matter on long TR/long TE images. This intensity pattern, also encountered in cystic and/or necrotic neoplasms, reflects the proteinaceous character of the abscess fluid with resultant T2 prolongation relative to brain and T1 shortening relative to CSF [9–11]. The development of mild hyperintensity on short TR/short TE images in the abscess cavity without interval change in intensity on long TR/intermediate to long TE images was seen in two early postoperative cases, and was possibly the result of intraoperative hemorrhage. Postoperative reduction in the size of the abscess cavity on MR (two of two cases studied serially; Figs. 5 and 6) correlated with similar changes on CT and with clinical improvement and, thus, was indicative of abscess healing [2].

One additional feature of the abscess cavity detected on long TR/intermediate to long TE scans in seven of 10 preoperative cases was the presence of concentric bands of varying intensity and thickness (Figs. 1D and 2E), a feature not encountered on MR in other cystic or necrotic lesions or on CT studies in this series, where the abscess cavity was uniformly hypodense (Fig. 1B) [12]. The cause of this MR finding is unknown. Pathologic studies have demonstrated necrotic debris without viable bacteria or host inflammatory cells; the consistency of the debris varies from a homogeneous liquid to nonuniform, disorganized, gelatinous material [13]. The findings on MR suggest a greater level of organization within the necrotic center than has been previously appreciated on CT (likely due to the greater sensitivity of MR)

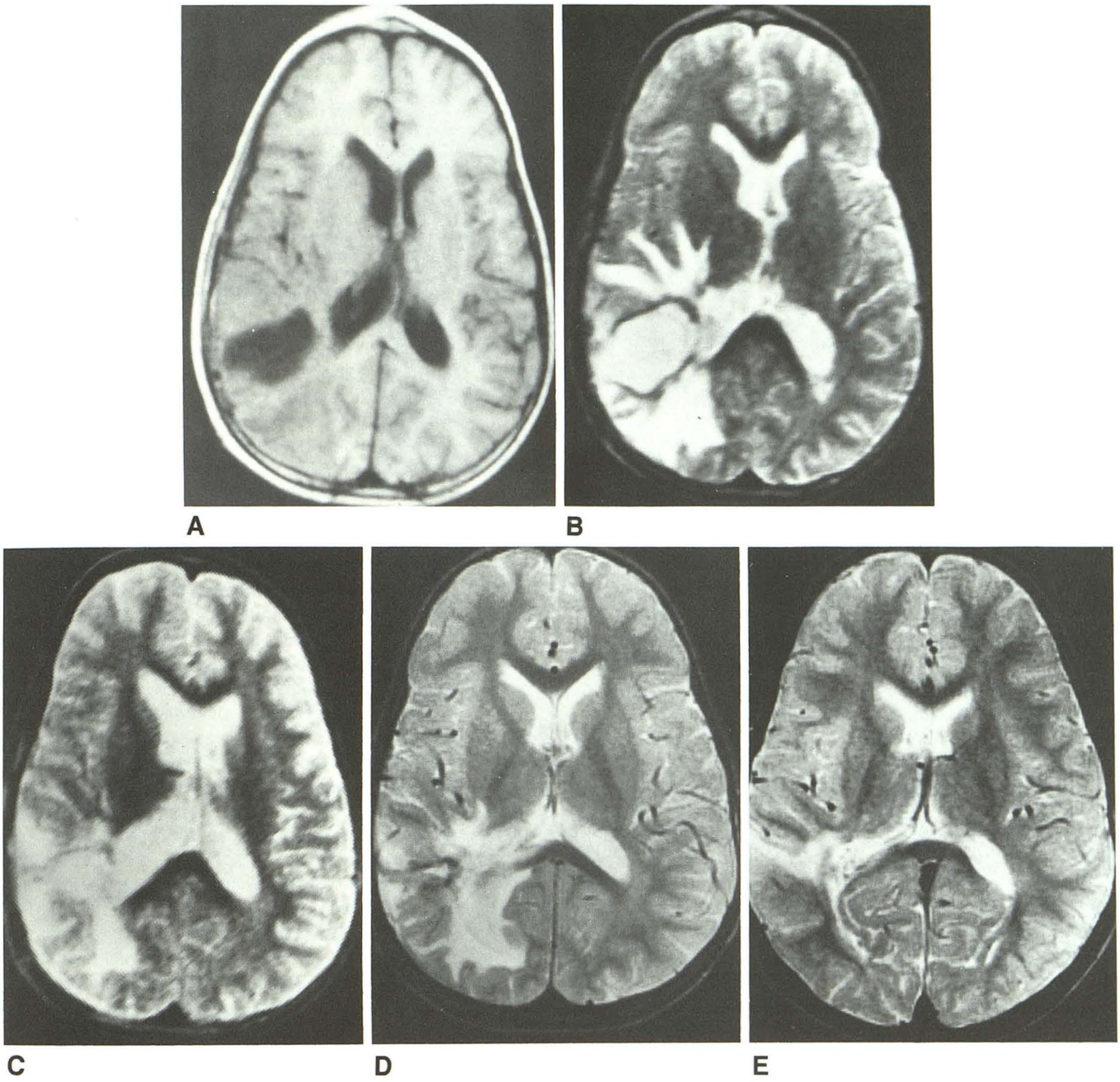

Fig. 6.—Case 1: Serial studies of postoperative brain abscess.

***A* and *B*, MR images, 500/32 (*A*) and 2150/120 (*B*), at 0.5 T 5 days after drainage of abscess show characteristic central fluid, edema, and rim intensities (grade II on 2150/120 scan).**

***C*, MR image, 2150/120, at 0.5 T 2 weeks after surgery shows decreased mass effect and rim hypointensity.**

***D*, MR image, 2000/80, at 1.5 T 6 weeks after surgery shows increase in rim hypointensity possibly related to increased sensitivity to magnetic susceptibility effects at higher field strength. Note collapse of abscess capsule.**

***E*, MR image, 2000/80, at 1.5 T 15 weeks after surgery shows resolution of mass effect and hypointense rim, with residual high intensity (probable gliosis and/or fibrosis).**

or at surgical or postmortem evaluation (possibly due to destruction of this organization by these invasive procedures).

Spread of inflammation into the ventricles and subarachnoid spaces is more conspicuous on MR than on CT. Extension into the quadrigeminal plate cistern (Fig. 1) and lateral ventricle (Fig. 3) resulted in hyperintensity in these spaces relative to CSF, especially on long TR/intermediate TE images, with no change in density on CT, reflecting the enhanced ability of MR to characterize proteinaceous fluids [9–11]. Extraparenchymal spread is an important differential diagnostic feature

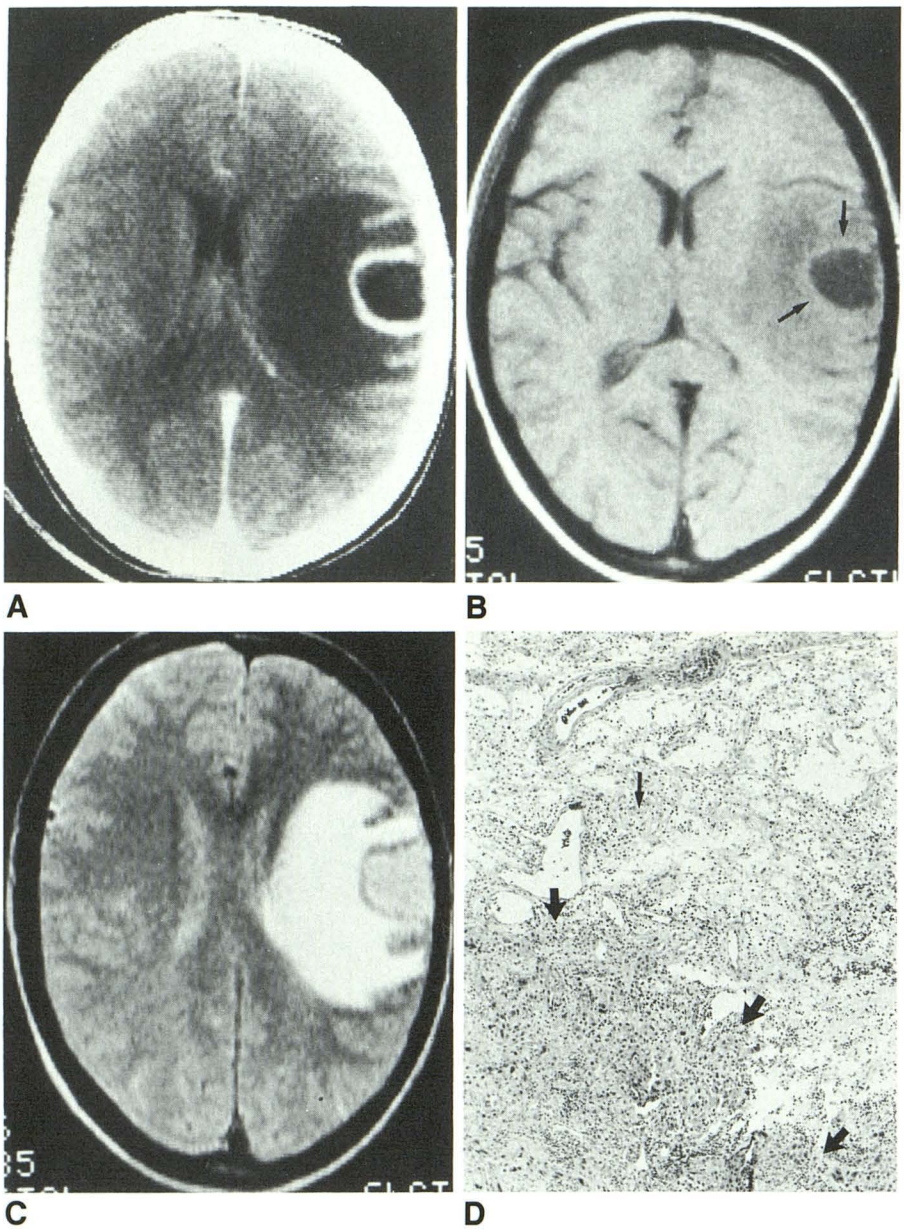

Fig. 7.—Metastatic papillary adenocarcinoma to left parietal lobe.

A, Contrast-enhanced CT scan shows ring enhancement, surrounding low-density edema, mass effect, and cortical location.

B, MR image, 500/32 (0.5 T), shows isointense rim (*arrows*) with adjacent hypointense peripheral edema and central necrosis.

C, MR image, 2150/96 (0.5 T), shows hyperintense central material, grade II intensity rim, and high-intensity surrounding edema.

D, Photomicrograph shows metastatic tumor (*large arrows*) surrounded by lipid-laden macrophages (*small arrow*), chronic inflammatory infiltrate, and numerous vessels. No evidence of acute or chronic hemorrhage or fibrosis is present. (H and E, original magnification × 63)

separating abscesses from other space-occupying lesions [2], and its detection has important therapeutic and prognostic implications.

A striking, unexpected, and clinically useful MR feature, noted in nine of 10 preoperative and four of four early postoperative cases, was the presence of a discrete rim interposed between the necrotic center and peripheral edema. The rim was iso- to mildly hyperintense relative to white matter on short TR/short TE images (Figs. 1C and 6A) and, more importantly, iso- to hypointense relative to white matter and hypointense relative to gray matter on long TR/intermediate to long TE images (Figs. 1D, 2C–2E, 5B, 5C, and 6B); Tables 2 and 3). This rim, present in all mature and chronic abscesses and absent only in the surgically and pathologically proved case of acute cerebritis, corresponded in location and configuration to the enhanced ring seen on CT. The rims were thin, smooth, and ovoid in contour, reflecting, as do CT rings, the unique pathology of abscess capsules and aiding differentiation from other lesions. Other characteristic CT findings duplicated by the dark rim on MR included gracile internal loculations and small satellite lesions (Figs. 1D, 2C, 2D, and 3B).

The rim on MR differed from the ring on CT in two respects, one morphologic and one temporal. Mesial wall thinning was more conspicuous on contrast-enhanced CT than on MR, though IV Gd-DTPA was able to duplicate this feature (Figs. 4B–4E). In the early postoperative period, decrease in the size of the rim on MR occurred simultaneously with decrease in size on CT (Fig. 5C). In the late postoperative period, however, rim resolution on MR preceded ring resolution on

CT. Because CT contrast enhancement may persist for at least 8 months after abscess healing [2, 14], rim resolution on MR may prove to be a more accurate assessment of healing.

Though a rim that is iso- to hypointense relative to white matter on long TR images occasionally may be seen in other lesions including subacute and chronic hematomas [15, 16], metastases [17], granulomatous lesions [18], and, rarely, gliomas [17], its presence in all abscesses studied and its uniform, circumferential appearance in each capsule are both unusual and noteworthy. Even extremely thin rim components such as satellite lesions were detected despite partial-volume effects from adjacent hyperintense edema and central necrosis (Figs. 1D and 3C). Normal white matter is hypointense relative to gray matter on long TR/intermediate to long TE images [9] (regions such as the splenium of the corpus callosum are nearly devoid of signal on long TR/long TE scans) because of decreased tissue water. In contrast, most intracerebral lesions are hyperintense relative to gray matter on long TR/intermediate to long TE images because of increased tissue water [19–24]. Thus, abscess rims that are either iso- or hypointense relative to white matter can be described as "hypointense" lesions, a term applied to some hematoma rims also [25] (Figs. 4E and 5B).

Various mechanisms were sought to explain the intensity pattern of the abscess rim that would be compatible with the observed pathologic and MR findings. Fibrosis and hemorrhage were initially considered likely causes. As expected, fibrous collagen was present in the mature abscess capsules [7, 13, 26] submitted for pathologic examination (Fig. 1E); however, the intensities of the rims did not match those seen in normal or pathologic intracranial fibrous tissue. Normal fibrous structures such as the falx and tentorium are hypointense on both short TR/short TE and long TR/intermediate to long TE images due to their low water and proportionately high protein content (Figs. 3B, 3C, and 4A–4C) [9, 10, 27], while the abscess rims are iso- to mildly hyperintense on short TR/short TE images. Pathologic fibrosis is rarely encountered intracranially, but several histologically proved examples of meningeal fibrosis demonstrated hyperintensity on long TR/intermediate to long TE images [28]. Furthermore, the temporal changes in rim intensity correlate poorly with the sequential changes of abscess healing. Specifically, deposition of collagen progresses with abscess maturation and persists after abscess resolution as a focal scar [13, 26]; thus, the dark rim should become progressively more prominent and persist with abscess healing. In fact, the rim showed only moderate (grade II) hypointensity in the most chronic preoperative abscesses (Cases 11 and 12, Fig. 5), and diminished and/or resolved on serial examinations in two patients studied 1 year after surgical drainage. Residual hyperintensity rather than hypointensity was seen in these two patients 1 year after successful treatment.

Though spontaneous hemorrhage into abscesses is rarely encountered clinically or documented pathologically [29], hemorrhage was considered a possible cause of the capsular intensities because of similarities to intensities seen in some stages of hematoma evolution. Thus, mild hyperintensity in the rim on short TR/short TE images may reflect paramagnetic proton-electron dipole-dipole interaction (T1 shortening) [9, 15], and hypointensity on long TR/intermediate to long TE images may reflect preferential T2 proton relaxation enhancement due to a heterogeneously distributed paramagnetic substance [15, 16, 30–32]. This capsular intensity pattern can be seen during the late acute stage of hemorrhage due to the presence of intracellular methemoglobin and/or a combination of extracellular methemoglobin and intracellular deoxyhemoglobin. In chronic hemorrhage, a hypointense rim, similar in appearance to the abscess rim, is seen because of the presence of hemosiderin-laden macrophages in the hematoma capsule [15, 30]. Support for the hypothesis that the intensities are due to paramagnetic T2 shortening comes from the findings of more pronounced hypointensity at 1.5 T than at 0.5 T (Cases 1 and 5) and the presence of hypointensity on gradient-echo pulse sequences [30].

However, careful review of our surgical reports and pathologic specimens showed no evidence of hemorrhage. Routine H and E stains (on which the presence of microscopic hemorrhage is commonly identified) showed no hemorrhage in the 10 cases in which specimens were available for review. Eight of these cases were restudied with Perls' stain for the presence of iron; no iron was found in six. The possibility that hemorrhage into the abscess capsule was missed due to the sampling error (e.g., only a small portion of the capsule was available for pathologic evaluation) seems unlikely since all but one of the biopsied rims were diffusely and relatively homogeneously hypointense. In the one inhomogenous rim (Fig. 2E), surgical notes confirmed that pathologic material was indeed obtained from a portion of the capsule with grade III intensity.

The presence of scant amounts of iron in two abscess capsules is unlikely to have been the primary cause of hypointensity on long TR images in these cases, because the degree of hypointensity did not correspond to the extent of iron deposition; that is, marked hypointensity (grade III) was seen in one case (Case 13, Fig. 1) while mild hypointensity (grade I) was seen in the other (Case 10, Fig. 4). In addition, scant amounts of iron are probably insufficient to cause hypointensity on long TR/intermediate to long images at 0.5 T, the field strength at which both patients were studied. Because preferential T2 shortening is, in part, dependent on field strength and the concentration of the intracellular paramagnetic substance [15, 33], small chronic hematomas often fail to produce discernible hypointensity on long TR spin-echo images at 0.5 T [34, 35]. In addition, careful histologic studies have revealed that lesions with scant hemorrhage may fail to demonstrate hypointensity on long TR/long TE images [19]. For instance, in Case 14 (Fig. 3), a scant amount of iron was microscopically identified in the choroid plexus, which was hyperintense on long TR/intermediate to long TE images, while the adjacent hypointense abscess rim did not contain iron.

Finally, the rapid temporal changes known to occur in hematoma intensity are difficult to reconcile with the constant intensity pattern in the abscess rim. In acute hemorrhage, hyperintensity on short TR/short TE images begins to develop

on approximately the third postictal day and persists for weeks to months, and hypointensity on long TR/intermediate to long images is transiently present from approximately the second to the 10th day [16, 32]. Thus, the combination of hyperintensity on short TR/short TE images and hypointensity on long TR/intermediate to long TE images, the pattern seen in abscess rims, is transiently present for approximately 1 week during hematoma evolution. However, the cases in this series were evaluated at various times after the onset of symptoms and at various pathologic stages of abscess evolution (Table 1), yet demonstrated a constant pattern of rim intensities. Furthermore, comparison of pre- and postoperative MR scans demonstrated no change in capsular intensities, with or without intraoperative hemorrhage (Case 12, Fig. 5). On the other hand, in the chronic stage, hemorrhage would be expected to demonstrate persistent hypointensity, particularly at high fields [15], in contrast to resolution of hypointensity seen with abscess healing at high fields (Case 10, Fig. 4; Case 1, Fig. 6).

Though hemorrhage is not the primary cause of the capsular intensities, the MR findings remain highly characteristic of paramagnetic T1 and T2 shortening. One possible source of a paramagnetic substance that heretofore has not been considered comes from the macrophages that are present in abundance in all abscess capsules (Table 3) [26]. In association with phagocytosis, macrophages (and neutrophils) undergo a respiratory burst, generating free radicals that destroy, or help destroy, the ingested microorganisms [36–38]. The initial step in this process is the conversion of molecular oxygen to the free radical superoxide, which then undergoes a variety of complex reactions to produce a large number of free radicals. For instance, the Haber-Weiss reaction converts superoxide to hydrogen peroxide, hydroxyl radical, and atomic oxygen. These free radicals, called reactive oxygen intermediates [38], are short-lived [39] and are generally detected by indirect biochemical methods, though they have been demonstrated by direct in vitro sampling of activated macrophages by electron spin resonance techniques [40–42].

These reactive oxygen intermediates differ in one major respect from paramagnetic substances more familiar to radiologists such as deoxyhemoglobin, methemoglobin, or melanin [19, 21] in that they are unstable and extremely short-lived. Therefore, capsular hypointensity cannot result from a single, easily measurable substance produced by a static group of cells, but rather (if this hypothesis is correct) from the continuous production of a string of short-lived free radicals generated during active phagocytosis by macrophages constantly entering the capsule from the vascular bed.

Another possible source of paramagnetic effects are the enzymes that catalyze these reactions [39]. For example, the Haber-Weiss reaction is catalyzed by copper and iron molecules, possibly in the form of nonheme paramagnetic proteins such as lactoferrin and transferrin [43], which are more stable than the reactive oxygen intermediates.

Certainly, this hypothesis will require extensive in vivo and in vitro evaluation, in particular to determine if activated macrophages and their associated respiratory burst are capable of producing detectable T1 and T2 shortening. Pending these evaluations, however, there is indirect evidence to support this hypothesis. First, pathologic evaluation of two metastatic foci with rim intensities mimicking those seen in abscesses revealed extensive macrophagic infiltrate in their rims (Fig. 7D). Except for these macrophages, no other histologic feature was common to both the metastases and the abscesses. Specifically, no fibrosis or hemorrhage was demonstrated in the metastases. Second, pathologic evaluation of the diffusely hypointense (on long TR scans) parenchymal tuberculoma demonstrated no fibrosis or hemorrhage, though macrophages were present in abundance. (Similar intensities have been reported in other tuberculomas [18, 44].)

Evaluation of the temporal changes in rim intensity also supports the hypothesis that hypointensity is a reflection of macrophage activity (host response). In the acute cerebritis stage, when the capsule is poorly formed, discrete hypointensity is not seen, and poorly defined hypointensity at this stage may reflect early macrophage reaction. In the early mature abscess stage, host response is maximal, as is the degree of hypointensity. In chronic untreated abscesses (Fig. 5), hypointensity is less marked, suggesting that the infection is partially contained and macrophage activity is waning. With treatment and healing, macrophage activity continues to decrease until hypointensity is no longer visualized (Figs. 4 and 6).

In conclusion, findings in 14 patients with pyogenic abscesses indicate a characteristic set of features that should allow for early and accurate diagnosis on MR. In addition, two important general conclusions seem warranted. First, intensities indicative of paramagnetic T1 and T2 shortening may be seen in the absence of hemorrhage. Second, the hypointense rim in pyogenic abscesses and possibly in other inflammatory lesions may prove to be an indicator of macrophage activity and, therefore, of host response. This may, in turn, have interesting implications for the experimental and clinical evaluation of these lesions and their therapy.

ACKNOWLEDGMENTS

We thank Anna Maria Giambruno and Luis Cintrone for preparation of special histopathologic slides.

REFERENCES

1. Rosenblum ML, Hoff JT, Norman D, Weinstein PR, Pitts L. Decreased mortality from brain abscesses since the advent of computerized tomography. *J Neurosurg* **1978**;49:658–668
2. Whelan MA, Hilal SK. Computed tomography as a guide in the diagnosis and follow-up of brain abscesses. *Radiology* **1980**;135:663–671
3. Claveria LE, du Boulay GH, Mosley IF. Intracranial infections: investigation by computerized tomography. *Neuroradiology* **1976**;12:54–71
4. Nielson H, Gyldensted C. Computed tomography in the diagnosis of cerebral abscess. *Neuroradiology* **1977**;12:207–217
5. Braun IF, Chambers E, Leeds NE, Zimmerman RD. The value of unenhanced scans in differentiating lesions producing ring enhancement. *AJNR* **1982**;3:643–647
6. Enzmann DR, Britt RH, Placone R. Staging of human brain abscess by computed tomography. *Radiology* **1983**;146:703–708
7. Enzmann DR. Focal parenchymal infection. In: Enzmann DR, ed. *Imaging*

of infections and inflammations of the central nervous system: computed tomography, ultrasound, and nuclear magnetic resonance. New York: Raven, **1984**:27–102
8. Holtas S, Tornquist C, Cronqvist S. Diagnostic difficulties in computed tomography of brain abscesses. *J Comput Assist Tomogr* **1982**;6(4): 683–688
9. Bradley WG Jr. Pathophysiologic correlates of signal alterations. In: Brant-Zawadzki M, Norman D, eds. *Magnetic resonance imaging of the central nervous system.* New York: Raven, **1987**:23–42
10. Mitchell DG, Burk DL Jr, Vinitski S, Rifkin MD. The biophysical basis of tissue contrast in extracranial MR imaging. *AJR* **1987**;149:831–837
11. Kjos BO, Brant-Zawadzki M, Kucharczyk W, et al. Cystic intracranial lesions: magnetic resonance imaging. *Radiology* **1985**;155:363–369
12. Danziger A, Price H, Schecter MM. An analysis of 113 intracranial infections. *Neuroradiology* **1980**;19:31–34
13. Alvord EC, Shaw C-M. Infectious, allergic, and demyelinating diseases of the nervous system. In: Newton TH, Potts DG, eds. *Radiology of the skull and brain*, Vol. 3. *Anatomy and pathology*, 1st ed. St. Louis: Mosby, **1977**:3088–3172
14. Dobkin JF, Healton EB, Dickinson PCT, Brust JCM. Nonspecificity of ring-enhancement in "medically cured" brain abscesses. *Neurology* **1984**;34:139–144
15. Gomori JM, Grossman RI, Goldberg HI, Zimmerman RA, Bilaniuk LT. Intracranial hematomas: imaging by high field MR. *Radiology* **1985**;157:87–93
16. Zimmerman RD, Heier LA, Snow RB, Liu DP, Kelly AB, Deck MDF. MR imaging features of acute intracranial hemorrhage studied at 0.5T with emphasis on sequential intensity changes on multiple pulse sequences. *AJNR* **1988**;9:47–57, *AJR* **1988**;150:651–661
17. Fleming CA, Zimmerman RD, Haimes A, Morgello S, Deck MDF. The diagnostic significance of rim intensity and edema patterns in the differentiation of intracranial mass lesions on MRI (abstr). *AJNR* **1987**;8:454
18. Gupta RK, Jena A, Sharma A, Guha DK, Khush S, Gupta AK. MR imaging of intracranial tuberculomas. *J Comput Assist Tomogr* **1988**;12(2): 280–285
19. Woodruff WW Jr, Diang WT, McLendon RE, Heinz ER, Voorhees DR. Intracerebral malignant melanoma: high-field-strength MR imaging. *Radiology* **1987**;165:209–213
20. Komiyama M, Yagura H, Baba M, et al. MR imaging: possibility of tissue characterization of brain tumors using T1 and T2 values. *AJNR* **1987**;8: 65–70
21. Brant-Zawadzki M. MR imaging of the brain. *Radiology* **1988**;166:1–10
22. Zimmerman RA, Bilaniuk LT, Johnson MH. MRI of central nervous system: early clinical results. *AJNR* **1986**;7:587–594
23. Lee BCP, Kneeland JB, Cahill PT, Deck MDF. MR recognition of supratentorial tumors. *AJNR* **1985**;6:871–878
24. Brant-Zawadzki M, Norman DC, Newton TH, et al. Magnetic resonance of the brain: the optimal screening technique. *Radiology* **1984**;152:71–77
25. Atlas SW, Grossman RI, Gomori JM, et al. Hemorrhagic intracranial malignant neoplasms: spin-echo MR imaging. *Radiology* **1987**;164:71–77
26. Robbins SL, Cotran RS, Kumar V. Inflammation and repair. In: Robbins SL, Cotran RS, Kumar V, eds. *Pathologic basis of disease*, 3rd ed. Philadelphia: Saunders, **1984**:40–84
27. Daniels DL, Pojunas KW, Kilgore DP. MR of diaphragma sellae. *AJNR* **1986**;7:765–769
28. Destian S, Heier LA, Zimmerman RD, Deck MDF. Meningeal fibrosis in patients with chronic ventriculoperitoneal shunts. Presented at the annual meeting of the American Society of Neuroradiology, Chicago, May **1988**
29. Bach D, Goldenberg MH. Hemorrhage into a brain abscess. *J Comput Assist Tomogr* **1983**;7(6):1067–1069
30. Edelman RR, Johnson K, Buxton R, et al. MR of hemorrhage: a new approach. *AJNR* **1986**;7:751–756
31. Zimmerman RD, Deck MDF. Intracranial hematomas: imaging by high field MR (letter). *Radiology* **1986**;159:565–566
32. Gomori JM, Grossman RI, Hackney DB, et al. Variable appearance of subacute intracranial hematomas on high-field spin-echo MR. *AJNR* **1987**;8:1019–1026
33. Thulborn KR, Waterton JC, Matthews PM, Radda CK. Oxygenation dependence of the transverse relaxation time of water protons in whole blood at high field. *Biochim Biophys Acta* **1982**;714:265–270
34. Zimmerman RD, Magnetic resonance imaging of intracranial hemorrhage. In: Sarwar M, Batnitzky S, eds. *Non-traumatic ischemia and hemorrhagic disorders of the CNS.* Boston: Martinus Nijhoff (in press)
35. Bradley WG Jr. MRI of hemorrhage and iron in the brain. In: Stark DD, Bradley WG Jr, eds. *Magnetic resonance imaging*. St. Louis: Mosby, **1988**:359–375
36. Eisen HN. Cell-mediated hypersensitivity and immunity. In: Davis BD, Dulbecco R, Eisen HN, Ginsberg HS, eds. *Microbiology, including immunology and molecular genetics*, 3rd ed. Hagerstown: Harper & Row, **1980**:494–521
37. Johnston RB Jr. Oxygen metabolism and the microbicidal activity of macrophages. *Fed Proc* **1978**;37:2759–2764
38. Adams DO, Hamilton TA. The cell biology of macrophage activation. *Annu Rev Immunol* **1984**;2:283–318
39. Southorn PA, Powis G. Free radicals in medicine: I. chemical nature and biologic reactions. *Mayo Clin Proc* **1988**;63:381–389
40. Hume DA, Gordon S, Thornalley PJ, Bannister JV. The production of oxygen-centered radicals by Bacillus-Calmette-Guérin-activated macrophages: an electron paramagnetic resonance study of the response to phorbol myristate acetate. *Biochim Biophys Acta* **1983**;763:245–250
41. Bannister JV, Bellavite P, Serra MC, Thornalley PJ, Rossi F. An EPR study of the production of superoxide radicals by neutrophil NADPH oxidase. *FEBS Lett* **1982**;145(2):323–326
42. Harbour JR, Bolton JR. Superoxide formation in spinach chloroplasts: electron spin resonance detection by spin trapping. *Biochim Biophys Res Commun* **1975**;64(3):803–807
43. Koenig SH, Schillinger WE. Nuclear magnetic relaxation dispersion in protein solution. II. Transferrin. *J Biol Chem* **1969**;244(23):6520–6526
44. Venger BH, Dion FM, Rouah E, Handel SF. MR imaging of pontine tuberculoma (letter). *AJNR* **1987**;8:1149–1150